

Unraveling the Origins and Development of the Galactic Disk through Metal-Poor Stars

Maria Rah ^{*1,2}, Manolya Yatman³, Ali Taani⁴, Ahmad A. Abushattal⁵, and Mohammad K. Mardini⁶

¹Byurakan Astrophysical Observatory, Armenia; R-PhD Student at BAO

²National Astronomical Observatory, Chinese Academy of Sciences, China; The Silk Road Project at NAOC

³Physics Department, Bryn Mawr College, 19010, Philadelphia, USA

⁴Physics Department, Faculty of Science, Al Balqa Applied University, 19117, Salt, Jordan

⁵Department of Physics, Al-Hussein Bin Talal University, P.O. Box 20, 71111, Ma'an, Jordan

⁶Department of Physics, Zarqa University, Zarqa 13110, Jordan

Abstract

The Milky Way is a spiral galaxy comprising three main components: the Bulge, the Disk, and the Halo. Of particular interest is the Galactic disk, which holds a significant portion of the baryonic matter angular momentum and harbors at least two primary stellar populations: the thin and thick disks. Understanding the formation and evolution of the Galactic disk is crucial for comprehending the origins and development of our Galaxy. Stellar archaeology offers a means to probe the disk's evolution by listening to the cosmological narratives of its oldest and most pristine stars, specifically the metal-poor stars. In this study, we employed accurate photometric metallicity estimates and Gaia Early Data Release 3 astrometry to curate a pure sample of the oldest Galactic stars. This proceeding presents a summary of our primary findings.

Keywords: *Early universe — Galaxy: dynamics — Galaxy: disc*

1. Introduction

The pioneering research carried out by [Gilmore & Reid \(1983\)](#) centered on investigating the stellar populations present in our Milky Way galaxy. The study extensively examined the motion and distribution of metals among stars, yielding valuable insights into the structure and evolution of our galaxy. An important discovery stemming from this research was the identification of distinct stellar groups, categorized according to their motion characteristics. These stars were divided into two main clusters: a thin disk population characterized by low velocity dispersion, and a thick disk population exhibiting higher velocity dispersion. This finding implies that diverse dynamic processes contributed to the formation and development of these two components. Furthermore, as stated by [Gilmore & Reid \(1983\)](#), both the thin and thick disk populations exhibited various metallicities; however, younger stars within the thin disk component generally displayed a preference for higher metallicity levels. This supports theories that suggest star formation in the Milky Way took place over a long period of time, and that subsequent generations of stars showed higher levels of enrichment with heavy elements. We have collected the key characteristics of these two distinct populations, as reported in literature and listed in [Table 1](#).

More recently, [Carollo et al. \(2019\)](#) identified two distinct modes of the Galactic thick-disk: “in-situ” and “ex-situ”. The in-situ population refers to the formation of stars within the Galactic disk, while the ex-situ population involves stars that were formed elsewhere and later accreted onto the our Galaxy. This component is referred to as the Metal-Weak Thick Disk. In this context, [Mardini et al. \(2022b\)](#) investigated the nature of this component by employing accurate photometric metallicity estimates and Gaia Early Data Release 3 astrometry ([Gaia Collaboration et al., 2023](#)). Furthermore, during the Gaia era, numerous studies have utilized these astrometry to yield essential constraints regarding the formation and evolution of our galaxy, the Milky Way ([Abu-Dhaim et al., 2022](#), [Chiti et al., 2021a,b](#), [Hong et al., 2023](#), [Mardini et al., 2022a, 2023](#), [Placco et al., 2023](#), [Zepeda et al., 2023](#)). In a nutshell, the study by [Mardini et al. \(2022a\)](#) offers

*E-mail: mariarah.astro@gmail.com, Corresponding author

Table 1. Orbital properties of the Galactic thin disk, thick disk, and inner halo

Parameter	unit	Thin disk	Thick disk	Inner halo	Atari disk
h_R	(kpc)	2.6 - 3.00	2.0 - 3.0	...	2.48 ± 0.05
h_Z	(kpc)	0.14 - 0.36	0.5 - 1.1	...	$1.68^{+0.19}_{-0.15}$
$\langle V_\phi \rangle$	(km s ⁻¹)	208	182	0	154 ± 1
Z_{max}	(kpc)	< 0.8	0.8 - 3.0	> 3.0	< 3.0
e	...	< 0.14	0.3 - 0.5	> 0.7	0.30 - 0.7

See [Mardini et al. \(2022b\)](#); and references therein.

significant insights into the formation and evolution of our Galaxy by emphasizing the spatial, kinematic, and chemical characteristics of this component, which suggest that multiple mechanisms contribute to Galactic disk growth.

2. Method and Analysis

We have developed two separate techniques, namely velocity and action space analysis, to initially select a pure sample of stars with $[\text{Fe}/\text{H}] \leq -0.8$ from the APOGEE-2/SDSS-IV dataset ([Blanton et al., 2017](#)). By displaying kinematics that are characteristic of the thick disk, our resulting sample consists of 90,000 stars with high-quality measurements of $[\text{Fe}/\text{H}]$ and astrometry. We then calculated the positions of our stars using the equations described in Equations 1. The velocity calculations were carried out according to Equation 2. In order to categorize our sample into the main Galactic components (i.e., Halo, thin disk, and thick disk), we defined velocity distributions as explained in Equation 3. The relative probabilities for the ratios between thick-disk-to-thin-disk (TD/D) and thick-disk-to-halo (TD/H) were determined using Equation 4. Each thick disk star was assigned with a membership probability of $\text{TD}/\text{D} > 2.0$, while stars with $\text{TD}/\text{D} < 0.5$ were classified as thin disk stars. Moreover, we excluded stars with $\text{TD}/\text{H} < 10.0$ to minimize potential contamination from the Galactic halo.

The above-mentioned method efficiently identifies stars exhibiting disk-like kinematics. Nonetheless, it is crucial to acknowledge that this approach might erroneously categorize halo stars, which have nearly-circular orbits and low orbital eccentricities, as disk-like stars (e.g., [Brauer et al., 2022](#), [Mardini et al., 2019a,b, 2020](#), [Placco et al., 2020](#)). To minimize the risk of contamination from the Galactic Halo, we have developed an alternative method that relies on stellar actions, as described by Equation 5. Furthermore, we utilized a spherically symmetric ad hoc approximation to evaluate the three distribution functions (DFs) individually, as outlined in Equation 6. The figure depicting the relative density distribution of each Galactic component, along with the dark matter profile, can be found in Figure 1. It is worth mentioning that the potential demonstrates a primarily isotropic characteristic (see [Almusleh et al., 2021](#), [Mardini et al., 2019c](#), [Taani et al., 2019a,b,c, 2020, 2022](#)). This yielded a sample of my 87075 stars, which spans a wide metallicity range.

3. Results and Conclusions

The average rotational velocity of our sample shows a 30 km s^{-1} lag compared to the well-known thick disk. To understand the origins of our sample stars, we analyze derived gradients, the shape of the eccentricity distribution, and theoretical scenarios for thick disk formation ([Abdusalam et al., 2020](#), [Al-Tawalbeh et al., 2021](#), [Al-Wardat et al., 2021](#), [Masda et al., 2019](#)). We also calculate the scale height and scale length of our sample using Equations 7, 8, 9, and 10. In terms of size, our sample is similar to the Galactic thick disk in the radial direction but has greater vertical extension. Furthermore, the distribution of orbital eccentricities in our sample bridges between those typically observed in the thick disk and halo populations. Our investigation into orbital eccentricities also reveals a significant number of stars with high eccentricities. These findings, combined with theoretical predictions, suggest that this population was introduced to our Galaxy through an early merger event involving the proto-Milky Way.

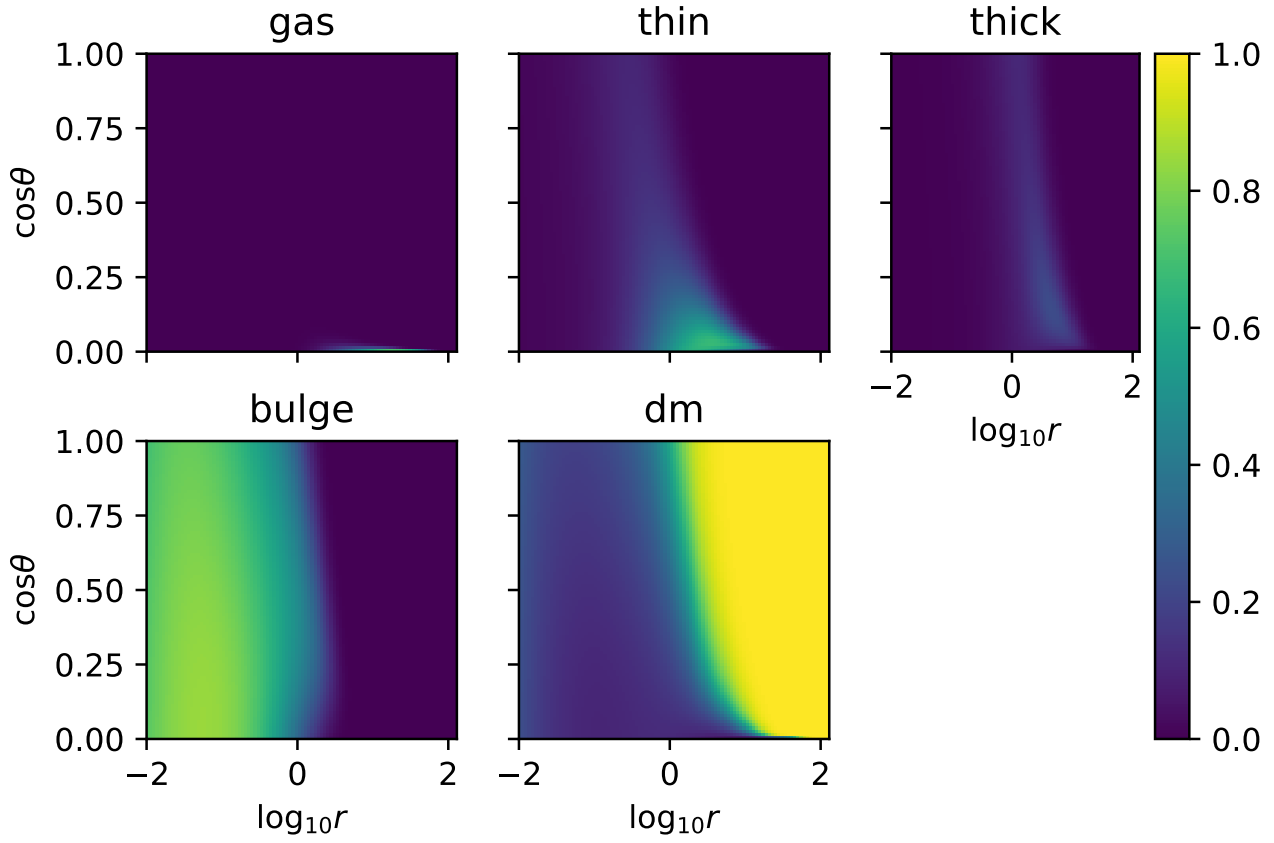


Figure 1. The relative density of each of the components.

$$\begin{aligned}
 X &= R_{\odot} - d \cos(l) \cos(b) \\
 Y &= -d \sin(l) \cos(b) \\
 Z &= d \sin(b)
 \end{aligned} \tag{1}$$

$$\begin{aligned}
 V_R &= U \cos \phi + (V + V_{rot}) \sin \phi \\
 V_{\phi} &= (V + V_{rot}) \cos \phi - U \sin \phi \\
 V_z &= W
 \end{aligned} \tag{2}$$

$$\begin{aligned}
 f(U, V, W) &= k \cdot \exp\left(-\frac{(V_{LSR} - V_{asym})^2}{2\sigma_V^2}\right. \\
 &\quad \left.-\frac{W_{LSR}^2}{2\sigma_W^2} - \frac{U_{LSR}^2}{2\sigma_U^2}\right)
 \end{aligned} \tag{3}$$

$$\begin{aligned}
 TD/D &= \frac{X_{TD} \cdot f_{TD}}{X_D \cdot f_D} \\
 TD/H &= \frac{X_{TD} \cdot f_{TD}}{X_H \cdot f_H}
 \end{aligned} \tag{4}$$

$$f_{halo}(J_r, J_z, L_z) = f_0 \left[1 + \frac{J_r + J_z + |L_z|}{J_0} \right]^{\beta_*} \tag{5}$$

$$\Phi_{approx}(r) = -\Phi_{0,fit} \frac{r_{fit}}{r} \left[1 - \frac{1}{(1 + r/r_{fit})^{\beta_{fit}-3}} \right] \tag{6}$$

$$\frac{\partial f}{\partial t} + v_R \frac{\partial f}{\partial R} + \frac{v_\phi}{R^2} \frac{\partial f}{\partial \phi} + v_z \frac{\partial f}{\partial z} - \left(\frac{\partial \Phi}{\partial R} - \frac{v_\phi^2}{R^3} \right) \frac{\partial f}{\partial v_R} - \frac{\partial \Phi}{\partial \phi} \frac{\partial f}{\partial v_\phi} - \frac{\partial \Phi}{\partial z} \frac{\partial f}{\partial v_z} = 0, \quad (7)$$

$$\rho K_Z = \frac{\partial(\rho \sigma_{V_Z}^2)}{\partial Z} + \frac{1}{R} \frac{\partial(R \rho \sigma_{V_{R,Z}}^2)}{\partial R} \quad (8)$$

$$\frac{\sigma_{V_\phi}^2}{\sigma_{V_R}^2} - 2 + \frac{2R}{h_R} - \frac{V_c^2 - \bar{V}_\phi^2}{\sigma_{V_R}^2} + \frac{\sigma_{V_Z}^2}{\sigma_{V_R}^2} = 0 \quad (9)$$

$$\frac{\partial \ln \sigma_{V_Z}^2}{\partial Z} - \frac{1}{h_Z} + \frac{K_Z}{\sigma_{V_Z}^2} = 0 \quad (10)$$

References

- Abdusalam K., Ablimit I., Hashim P., Lü G. L., Mardini M. K., Wang Z. J., 2020, *Astrophys. J.* , **902**, 125
- Abu-Dhaim A., Taani A., Tanineah D., Tamimi N., Mardini M., Al-Wardat M., 2022, *Acta Astronomica.* , **72**, 171
- Al-Tawalbeh Y. M., et al., 2021, *Astrophysical Bulletin*, **76**, 71
- Al-Wardat M. A., et al., 2021, *Research in Astronomy and Astrophysics*, **21**, 161
- Almusleh N. A., Taani A., Özdemir S., Rah M., Al-Wardat M. A., Zhao G., Mardini M. K., 2021, *Astronomische Nachrichten*, **342**, 625
- Blanton M. R., et al., 2017, *Astron. J.* , **154**, 28
- Brauer K., Andales H. D., Ji A. P., Frebel A., Mardini M. K., Gómez F. A., O'Shea B. W., 2022, *Astrophys. J.* , **937**, 14
- Carollo D., et al., 2019, *Astrophys. J.* , **887**, 22
- Chiti A., Frebel A., Mardini M. K., Daniel T. W., Ou X., Uvarova A. V., 2021a, *Astrophys. J. Suppl. Ser.* , **254**, 31
- Chiti A., Mardini M. K., Frebel A., Daniel T., 2021b, *Astrophys. J. Lett.* , **911**, L23
- Chiti A., et al., 2023, *Astron. J.* , **165**, 55
- Gaia Collaboration et al., 2023, *Astron. Astrophys.* , **674**, A1
- Gilmore G., Reid N., 1983, *mnras*, **202**, 1025
- Hong J., et al., 2023, *arXiv e-prints*, p. [arXiv:2311.02297](https://arxiv.org/abs/2311.02297)
- Mardini M. K., et al., 2019a, *The Astrophysical Journal*, **875**, 89
- Mardini M. K., Placco V. M., Taani A., Li H., Zhao G., 2019b, *The Astrophysical Journal*, **882**, 27
- Mardini M. K., Ershiadat N., Al-Wardat M. A., Taani A. A., Özdemir S., Al-Naimiy H., Khasawneh A., 2019c, in *Journal of Physics Conference Series*. p. 012024 ([arXiv:1904.09608](https://arxiv.org/abs/1904.09608)), [doi:10.1088/1742-6596/1258/1/012024](https://doi.org/10.1088/1742-6596/1258/1/012024)
- Mardini M. K., et al., 2020, *The Astrophysical Journal*, **903**, 88
- Mardini M. K., et al., 2022a, *Mon. Not. R. Astron. Soc.* , **517**, 3993
- Mardini M. K., Frebel A., Chiti A., Meiron Y., Brauer K. V., Ou X., 2022b, *Astrophys. J.* , **936**, 78
- Mardini M. K., Frebel A., Betre L., Jacobson H., Norris J. E., Christlieb N., 2023, *arXiv e-prints*, p. [arXiv:2305.05363](https://arxiv.org/abs/2305.05363)
- Masda S. G., Docobo J. A., Hussein A. M., Mardini M. K., Al-Ameryeen H. A., Campo P. P., Khan A. R., Pathan J. M., 2019, *Astrophysical Bulletin*, **74**, 464
- Placco V. M., et al., 2020, *Astrophys. J.* , **897**, 78
- Placco V. M., et al., 2023, *arXiv e-prints*, p. [arXiv:2310.17024](https://arxiv.org/abs/2310.17024)
- Taani A., Karino S., Song L., Al-Wardat M., Khasawneh A., Mardini M. K., 2019a, *Research in Astronomy and Astrophysics*, **19**, 012
- Taani A., Abushattal A., Mardini M. K., 2019b, *Astronomische Nachrichten*, **340**, 847
- Taani A., Karino S., Song L., Mardini M., Al-Wardat M., Abushattal A., Khasawneh A., Al-Naimiy H., 2019c, in *Journal of Physics Conference Series*. p. 012029, [doi:10.1088/1742-6596/1258/1/012029](https://doi.org/10.1088/1742-6596/1258/1/012029)
- Taani A., Khasawneh A., Mardini M., Abushattal A., Al-Wardat M., 2020, *arXiv e-prints*, p. [arXiv:2002.03011](https://arxiv.org/abs/2002.03011)
- Taani A., Vallejo J. C., Abu-Saleem M., 2022, *Journal of High Energy Astrophysics*, **35**, 83
- Zepeda J., et al., 2023, *Astrophys. J.* , **947**, 23
- Maria Rah et al.
doi: <https://doi.org/10.52526/25792776-23.70.2-306>